

Electrical conduction mechanism in $\text{Se}_{90-x}\text{Te}_5\text{Sn}_5\text{In}_x$ ($x = 0, 3, 6$ and 9) multi-component glassy alloys

Cite as: AIP Advances 5, 087164 (2015); <https://doi.org/10.1063/1.4929577>

Submitted: 15 June 2015 . Accepted: 13 August 2015 . Published Online: 21 August 2015

Indra Sen Ram , Sunil Kumar, Rajesh Kumar Singh , Prabhakar Singh, and Kedar Singh



View Online



Export Citation



CrossMark

ARTICLES YOU MAY BE INTERESTED IN

Temperature dependent electrical transport characteristics of BaTiO_3 modified lithium borate glasses

AIP Advances 5, 087110 (2015); <https://doi.org/10.1063/1.4928339>

Electrical and optical properties of n-type semiconducting chalcogenide glasses in the system Ge-Bi-Se

Journal of Applied Physics 51, 1048 (1980); <https://doi.org/10.1063/1.327710>

Temperature and frequency dependent conductivity of bismuth zinc vanadate semiconducting glassy system

Journal of Applied Physics 112, 083701 (2012); <https://doi.org/10.1063/1.4759356>

AVS Quantum Science

Co-Published by



RECEIVE THE LATEST UPDATES

AIP
Publishing

Electrical conduction mechanism in $\text{Se}_{90-x}\text{Te}_5\text{Sn}_5\text{In}_x$ ($x = 0, 3, 6$ and 9) multi-component glassy alloys

Indra Sen Ram,¹ Sunil Kumar,² Rajesh Kumar Singh,³ Prabhakar Singh,³ and Kedar Singh^{4,5,a}

¹Department of Physics, Dyal Singh College (University of Delhi), New Delhi-110003, India

²Department of Physics, Dr. R. M. L. Government Degree College, Bareilly-243301, India

³Department of Physics, Indian Institute of Technology (Banaras Hindu University), Varanasi-221005, India

⁴Department of Physics, Banaras Hindu University, Varanasi-221005, India

⁵School of Physical Science, Jawaharlal Nehru University, New Delhi-110067, India

(Received 15 June 2015; accepted 13 August 2015; published online 21 August 2015)

Electrical conductivity of $\text{Se}_{90-x}\text{Te}_5\text{Sn}_5\text{In}_x$ ($x = 0, 3, 6$ and 9) glassy systems was studied employing impedance spectroscopic technique in the frequency range 100 Hz to 1 MHz and in the temperature range 308-388 K. The DC conductivity (σ_{dc}) at each temperature was evaluated from the low frequency plateau region for all the samples under investigation. The bulk conductivity for each sample was also evaluated from Nyquist impedance plots. The semicircle shape of Nyquist plot exhibit dipolar nature of samples. The activation energy for glassy, amorphous and crystalline region from the Arrhenius plot of the DC conductivity and bulk conductivity was evaluated. From the results it is found that activation energy varied from 0.091 to 0.194 eV in glassy, 0.686 to 0.002 eV in amorphous and 0.215 to 0.503 eV in crystalline region. The activation energy (ΔE) from DC conductivity and bulk conductivity found to be close in corresponding regions. The pre-exponential factor was also calculated for all three regions. © 2015 Author(s). All article content, except where otherwise noted, is licensed under a Creative Commons Attribution 3.0 Unported License. [<http://dx.doi.org/10.1063/1.4929577>]

I. INTRODUCTION

Chalcogenide glasses are semiconductor materials which have a wide variety of applications in electronic industry. The physical properties like structural, electrical, optoelectronic, etc. of materials can be controlled by altering their chemical compositions. The electrical properties of selenium (Se) based chalcogenide glasses have received attention because of its successful applications.¹⁻¹⁰ Due to unique reversible transformation properties amorphous Se has wide commercial applications.¹¹ But, pure Se has disadvantages owing to its short lifetime and low photosensitivity. To overcome these problems certain additives (e.g. Te, Sn, In, Sb etc.) are used to prepare binary glassy systems. These binary glassy systems have greater hardness, higher photosensitivity, higher crystallization temperature and smaller ageing effect as compared to pure amorphous Se.¹² The various physical properties of binary glassy system further can be enhanced by adding a third element as a chemical modifier. These physical properties can be more precisely tuned by adding fourth element in ternary glassy system. Therefore, quaternary glassy system is of vast importance. In this regard, the studies of various physical properties of chalcogenide glasses have become significant.

The various workers have synthesized and studied different physical properties of quaternary glassy systems.¹³⁻²² The glass transition and crystallization kinetics of $\text{Se}_{90-x}\text{Te}_5\text{Sn}_5\text{In}_x$ system were studied by our group and results are published elsewhere.^{20,21} The thermal transport properties of the discussed system are also studied.²²

^aCorresponding author: Email address: kedarbhp@rediffmail.com (K. Singh)

The electrical and dielectric properties of chalcogenide glasses are of great importance and had been studied by various workers.^{23–30} To the best of our knowledge electrical and dielectric properties of this system are not yet been studied. In the present study, we measured the electrical conductivity of $\text{Se}_{90-x}\text{Te}_5\text{Sn}_5\text{In}_x$ ($x = 0, 3, 6$ and 9) glassy systems in the frequency range 100 Hz - 1 MHz and temperature range 308–388 K. The dependence of electrical conductivity with concentration as well as frequency and temperature are discussed. The bulk conductivity is evaluated from impedance plots. The activation energy ΔE is evaluated from the Arrhenius plot of the DC conductivity as well as of the Bulk conductivity and is found to be close in the corresponding region. The pre-exponential factor is also evaluated and discussed for all the samples under investigation.

II. EXPERIMENTAL DETAILS

The investigated glasses were prepared from high purity (99.999%) Se, Te, Sn and In elements by the melting and quenching technique. The alloying elements were weighed according to their atomic weight percentage and mixtures were put into cleaned quartz ampoules. The ampoules were sealed under a vacuum of 10^{-5} Torr to prohibit any reaction of alloying elements with oxygen at higher temperature. The bunch of sealed ampoules was heated in a furnace at the rate of 3–4 K / min, the temperature was raised up to 1098 K and kept constant for 12 hrs. Throughout the melting process, the ampoules were frequently shaken to ensure the homogeneity of alloying materials. After the above said period, the ampoules with molten materials were rapidly quenched into ice-cooled water. The prepared glassy materials were taken out from the ampoules by breaking them. The amorphous and glassy natures of prepared samples were confirmed from X-ray diffraction patterns and DSC.^{20,21} Electrical conductivity measurements were performed employing high frequency digital LCR Meter -Wayne Kerr 6500 P Series in the frequency range 100 Hz to 1 MHz and the temperature range 308–388 K. For this, the samples were pressed into cylindrical pellet forms having diameter 10 mm and thickness of about 1.0 mm under uniform load of 5 tons using hydraulic press. A pellet was sandwiched between two circular silver discs in order to ensure good electrical contact between sample and electrodes of the LCR meter. This whole assembly of sample and discs is placed between the electrodes of the LCR meter. The electrical conductance G and dielectric loss $\tan(\delta)$ were measured at various temperatures and frequencies. The electrical conductivity and impedance parameters were calculated from measured values of G and $\tan(\delta)$.

III. RESULTS AND DISCUSSION

To study the variation of electrical conductivity with frequency at different temperature for samples under investigation, we show conductivity spectra of $\text{Se}_{87}\text{Te}_5\text{Sn}_5\text{In}_3$ glass as representative plot in Fig. 1. Other glass samples show similar behavior at different temperatures, moreover, Fig. 2 shows frequency dependent conductivity for different compositions at temperature $T = 308$ K. in. From Fig. 1 and Fig. 2, we can see that each sample has two regions, a frequency independent region in low frequency regime and a frequency as well as the temperature-dependent region in higher frequency regime. The frequency independent region in low frequency range can be assigned as DC conductivity and frequency dependent dispersion region can be assigned to the hopping motion or AC conductivity of the system. This is well known that DC conduction arises due to random hopping motion of charge carriers and AC dispersion region arises due to forward backward correlated hopping motion of charge carriers.³¹ It is clear from Fig. 2 that DC conductivity initially decreases after incorporation of In in Se-Te-Sn system at the cost of Se for 3 at wt % of In, again dc conductivity increases with increasing In content. This can be explained on the basis of structural change due to incorporation of In in Se-Te-Sn glassy system. Usually, accepted structural model for amorphous Se includes two molecular class,³² meandering chains containing helical chains of trigonal Se and Se_8 ring of monoclinic Se. The structure of the Se–Te system^{32–35} prepared by melting and quenching is regarded as a mixture of Se_8 rings, Se_6Te_2 rings and Se–Te copolymer chains. The addition of Sn in Se–Te system changes the structure by forming Sn–Te cubic and SnSe_2 tetrahedral phase and decreases the proportion of Se_8 rings. When In is incorporated in Se–Te–Sn, it satisfies the coordination requirement for making bonds with Se atoms by forming Sn–Te cubic and SnSe_2 tetrahedral phase and is probably dissolved

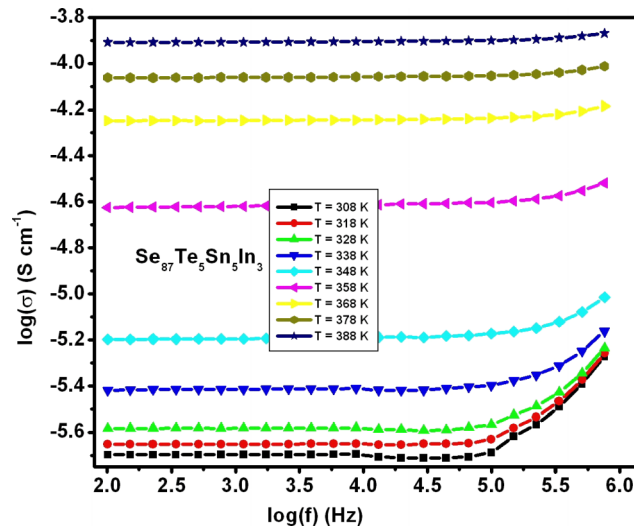


FIG. 1. The variation of electrical conductivity with frequency at different temperature of $\text{Se}_{87}\text{Te}_5\text{Sn}_5\text{In}_3$ glass.

in the Se rings.^{20,22} The formation of ionocovalent bond of In with Se in addition to covalent bond for higher at wt % (> 3 at wt %) of In may cause further increase in dc conductivity.³⁶

Further, the onset of cross-over frequency for AC dispersion increases with increasing temperature for all glasses under investigations. Since, with increasing temperature the probability of random hopping motion increases, therefore the onset of dispersion region increases with increasing temperature. Fig. 2 depicts that $\text{Se}_{90}\text{Te}_5\text{Sn}_5$ has almost DC conduction region in observed frequency range. This happens due to higher cross-over frequency for $\text{Se}_{90}\text{Te}_5\text{Sn}_5$ glass, which may be above the highest frequency range measured by equipment. It is known that d.c. conductivity arises due to band conduction and the a.c. conductivity arises due to relaxation processes. Further, d.c. and a.c. conductivities are due to different mechanisms depending on band gap and defect concentrations.³⁷ Thus, the onset of cross-over frequency depends on band gap as well as defect concentrations. Also, the onset of cross-over frequency decreases with In concentration up to 3 at wt %. This decrease may be due to the increase in no. of defects by incorporation of In in Se-Te-Sn system. However, this cross over frequency increases with further In addition (more than 3 at wt %) may be due to formation of ionocovalent bond of In with Se, which may change band gap.

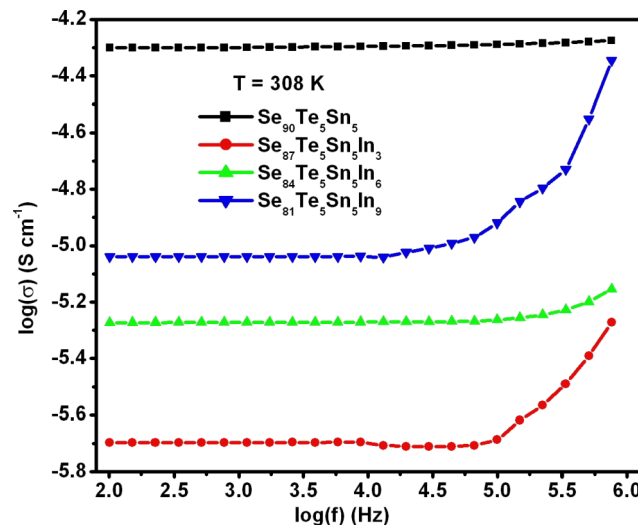


FIG. 2. The variation of electrical conductivity with frequency for different compositions at temperature $T = 308$ K.

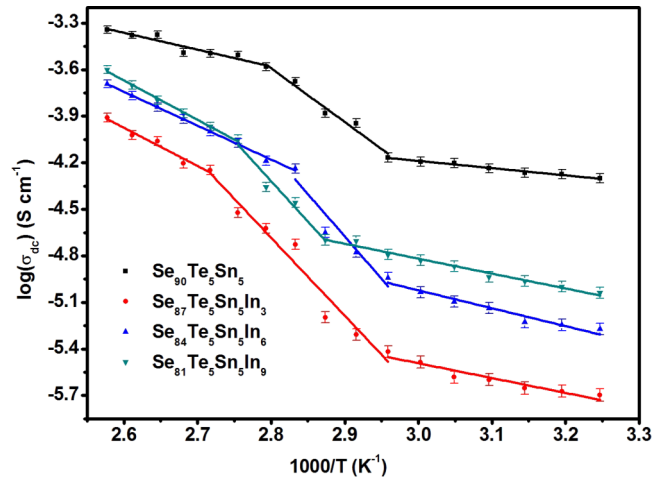


FIG. 3. The plots of $\log(\sigma_{dc})$ versus $1000/T$ for $\text{Se}_{90-x}\text{Te}_5\text{Sn}_5\text{In}_x$ ($x = 0, 3, 6$ and 9) glassy system.

The frequency dependent conductivity, in present case, can be described in terms of Johnson power law³⁸ $\sigma(f) = \sigma_{dc} + A.f^s$, where, σ_{dc} and A are associated with thermal activation and s is the frequency exponent.

The DC conductivity (σ_{dc}) at each temperature is also evaluated from the low frequency plateau region for all the samples under investigation. The temperature dependence of DC conductivity for $\text{Se}_{90-x}\text{Te}_5\text{Sn}_5\text{In}_x$ ($x = 0, 3, 6$ and 9) glassy systems is shown in Fig. 3 in Arrhenius representation. The graphs of $\log(\sigma_{dc})$ versus $1000/T$, can clearly be divided into three characteristic regions for all samples. This behavior may be attributed to the phase transformation with temperature. Earlier studies on these samples^{20,21} confirm that these glasses have three regions, (i) glassy region from room temperature to glass transition temperature T_g , (ii) amorphous region from T_g to crystallization temperature T_c , and (iii) crystalline region from T_c onwards. It is clear from the DSC thermograms^{20,21} of these samples that as temperature increases each material changes from its glassy state to amorphous state by absorbing heat around T_g and amorphous state to crystalline state by ejecting heat around T_c . In general, solids are found or synthesized either in a crystalline (ordered) state or in an amorphous (disordered) state. The crystalline solid possesses seven structural forms and possesses long range order; alternatively, an amorphous solid is neither unique nor clearly defined and possesses short range order. In amorphous solids, the materials exhibiting glass transition temperature are known as glassy materials and also called super cooled liquid. All glassy materials are amorphous material, but converse is not true. The entropy of material in glassy region is less than that in amorphous region.

The DC conductivity σ_{dc} can be expressed in these three regions by usual Arrhenius relation as;

$$\sigma_{dc} = \sigma_0 \exp(-\Delta E_{dc}/kT) \quad (1)$$

Where, ΔE_{dc} is the activation energy for DC conduction, k is Boltzman constant, σ_0 is the pre-exponential factor and T is absolute temperature. The activation energy (ΔE_{dc}) is evaluated by measuring the slope of straight line in the Fig. 3. All the investigated glasses show three activation energies corresponding to three conduction regions as shown in Fig. 3. The values of ΔE_{dc} for different samples

TABLE I. The variation of ΔE_{dc} and σ_0 $\text{Se}_{90-x}\text{Te}_5\text{Sn}_5\text{In}_x$ ($x = 0, 3, 6$ and 9) glassy system.

S. No.	Sample	ΔE_{dc} (eV)			$\sigma_0(\Omega^{-1}\text{cm}^{-1})$		
		Region(I)	Region(II)	Region(III)	Region(I)	Region(II)	Region(III)
1.	$\text{Se}_{90}\text{Te}_5\text{Sn}_5$	0.092	0.691	0.215	16.2×10^{-2}	1.51×10^6	0.30
2.	$\text{Se}_{87}\text{Te}_5\text{Sn}_5\text{In}_3$	0.188	0.994	0.486	22.7×10^{-2}	2.37×10^9	255.0
3.	$\text{Se}_{84}\text{Te}_5\text{Sn}_5\text{In}_6$	0.200	0.875	0.436	2.61×10^{-2}	6.02×10^{10}	85.5
4.	$\text{Se}_{81}\text{Te}_5\text{Sn}_5\text{In}_9$	0.190	1.022	0.500	1.14×10^{-2}	1.36×10^{10}	796.0

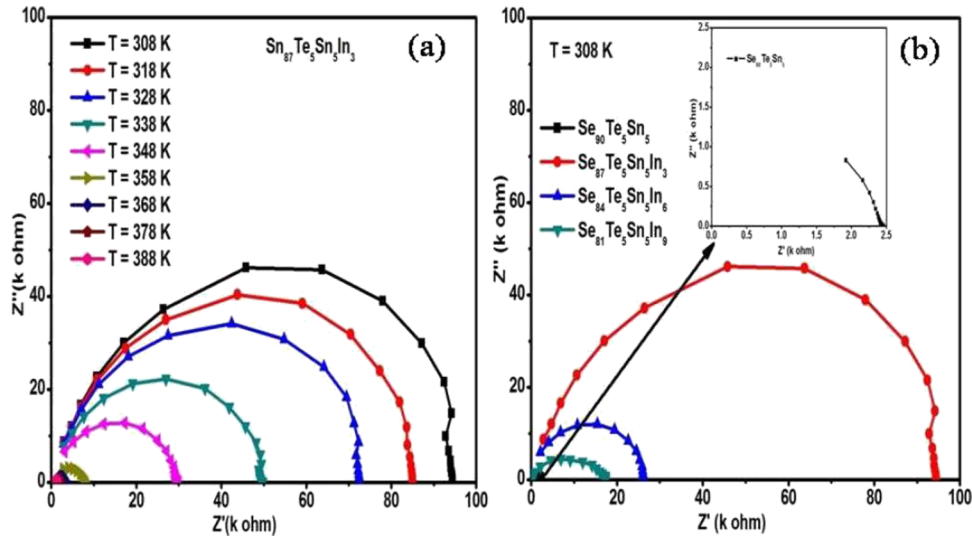


FIG. 4. The plots of Z'' (imaginary part of impedance) versus Z' (real part of impedance) for (a) $\text{Se}_{87}\text{Te}_5\text{Sn}_5\text{In}_3$ glass at different temperature, (b) different compositions at temperature $T = 308$ K.

in different regions are listed in Table I. Also, the values of pre-exponential factor σ_0 for different samples in different regions are listed in this table I. The activation energy alone cannot decide the nature of conduction mechanism because of co-existence of conduction in band tails and conduction in extended states. The pre-exponential factor is an important parameter to decide nature of conduction mechanism in amorphous semiconductors.^{39,40} The values of σ_0 for a-Se and Se based chalcogenide glasses is expected to be of the order of $10^4 \Omega^{-1}\text{cm}^{-1}$ for conduction in the extended states.³⁹⁻⁴¹ The lower value of σ_0 (2 or 3 order smaller than above mentioned value) represents the conduction in localized states present in band tails and still lower value corresponds to the conduction in localized states near the Fermi level.^{39,42} From the obtained values of ΔE_{dc} and σ_0 , it can be observed that conduction mechanism changes from conduction in band tails to conduction in extended states, again with increasing temperature conduction comes in band tails.

Bulk conductivity of $\text{Se}_{90-x}\text{Te}_5\text{Sn}_5\text{In}_x$ ($x = 0, 3, 6$ and 9) glassy system is evaluated by using the complex impedance technique.⁴³ The measurements were carried out in temperature range 308-388 K and frequency range 100 Hz - 1MHz. The plots of Z'' (imaginary part of impedance) versus Z' (real part of impedance) for $\text{Se}_{87}\text{Te}_5\text{Sn}_5\text{In}_3$ glass are shown in Fig. 4(a). The plots of Z'' versus Z' for other

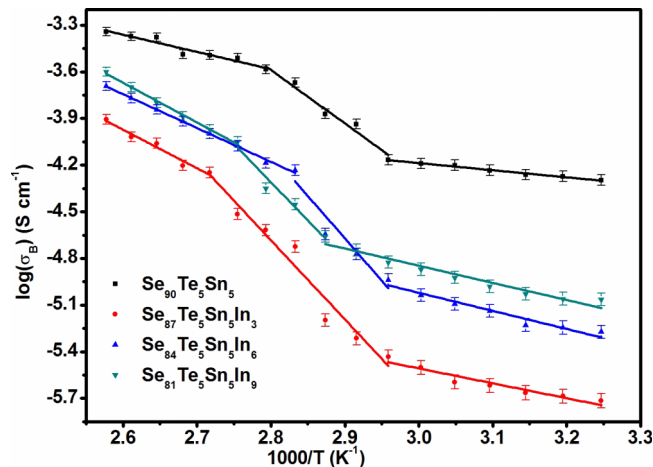


FIG. 5. The plots of $\log(\sigma_B)$ versus $1000/T$ for $\text{Se}_{90-x}\text{Te}_5\text{Sn}_5\text{In}_x$ ($x = 0, 3, 6$ and 9) glassy system.

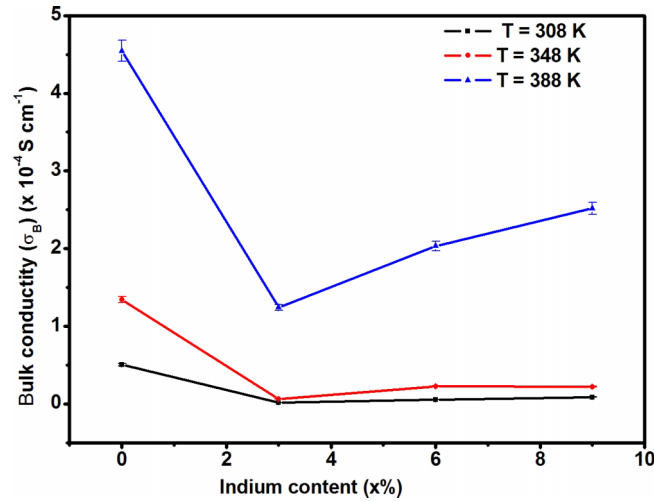


FIG. 6. The variation of bulk conductivity σ_B with In content at three different temperatures ($T = 308$ K, $T = 348$ K and $T = 388$ K).

samples have shown similar behavior (not shown in figure). The plots of Z'' versus Z' for different compositions at temperature $T = 308$ K shown in Fig. 4(b). The impedance plots for each investigated sample appear in the form of a semicircle at various temperatures. This results show that all samples have dipolar nature. The intersection of the semicircle at lower frequency with Z' -axis gives the bulk resistance (R_B) of the sample. It is also clear from Fig. 4(a) that diameter of semicircle decreases with the increase in temperature, consequently DC conductivity increases. The bulk conductivity of each sample at different temperature is calculated by using formula, $\sigma_B = t/(R_B A)$, t = thickness of sample, A = area of sample and R_B is bulk resistance. The variation of bulk conductivity σ_B with In content at three different temperature is shown in Fig. 6. At $T = 308$ K and $T = 348$ K, σ_B decreases with In content up to 3 at wt %, after that σ_B increases very slowly with higher concentration of In. Moreover, at $T = 388$ K, σ_B decreases with In content up to 3 at wt %, after that σ_B again increases with higher concentration of In. This result indicates that In concentration above 3 at wt % does not significantly affect the bulk conductivity in glassy and amorphous region as 308 K and 348 K corresponds to glassy and amorphous region, respectively; but In affects bulk conductivity at all concentration levels in region where crystallization just starts. When In is incorporated in Se–Te–Sn system, different phases of InSe (e.g. InSe, In_2Se_3 , In_5Se_6 , In_6Se_7) are formed. It is reported that the electrical resistance decreases up to 10^6 times of In_2Se_3 thin film in crystalline state.⁴⁴ The drastic decrease in electrical resistance of InSe phase occurs due to crystallization; therefore, Indium concentration affects bulk conductivity significantly in crystallization region. The plots of $\log(\sigma_B)$ versus $1000/T$ for $\text{Se}_{90-x}\text{Te}_5\text{Sn}_5\text{In}_x$ ($x = 0, 3, 6$ and 9) glassy system is shown in Fig. 5.

Also, activation energy for bulk conduction is evaluated by using Arrhenius type relation as;

$$\sigma_B = \sigma_0' \exp(-\Delta E_B/kT) \quad (2)$$

Where, ΔE_B is the activation energy for bulk conduction and other symbols has their usual meanings. The values of ΔE_B for different samples are listed in Table II. These values are also having the

TABLE II. The variation of ΔE_B and σ_0 $\text{Se}_{90-x}\text{Te}_5\text{Sn}_5\text{In}_x$ ($x = 0, 3, 6$ and 9) glassy system.

S. No.	Sample	ΔE_B (eV)		
		Region(I)	Region(II)	Region(III)
1.	$\text{Se}_{90}\text{Te}_5\text{Sn}_5$	0.091	0.686	0.219
2.	$\text{Se}_{87}\text{Te}_5\text{Sn}_5\text{In}_3$	0.188	1.008	0.489
3.	$\text{Se}_{84}\text{Te}_5\text{Sn}_5\text{In}_6$	0.200	0.879	0.430
4.	$\text{Se}_{81}\text{Sn}_5\text{Te}_5\text{In}_9$	0.194	0.965	0.503

same trend as obtained by DC conduction. The values of ΔE_B and ΔE_{dc} in corresponding regions are approximately same within experimental error. From this, we can conclude that DC conduction in investigated glassy system is mainly due to bulk conduction. The other sources of dc conductivity besides bulk are grain boundary and interface with electrodes.

IV. CONCLUSIONS

Conduction mechanism changes from conduction in band tails to conduction in extended states, again with increasing temperature conduction becomes in band tails. Semicircle appeared in the impedance plots show that all samples have dipolar nature. The values of activation energy for bulk conduction and DC conduction in corresponding regions are approximately same within experimental error. DC conduction in investigated glassy system is mainly due to bulk conduction.

ACKNOWLEDGEMENT

K S is thankful to Department of Science and Technology (SR/FTP/PS-200/2012) and University Grant commission (No. 42-812/ 2013(SR)) for providing financial support.

- ¹ D. Adler, M. Shur, M. Silver, and S. Ovshinsky, *J. Appl. Phys* **51**, 103 (1980).
- ² M. Chen, K. Rubin, and R. Barton, *Appl. Phys. Letter* **49**, 502 (1986).
- ³ N Yamada, E. Ohno, K. Nishiuchi, N. Akahira, and M Takao, *J. Appl. Phys* **69**, 2849 (1991).
- ⁴ A. Jongenelis, W. E. Spiekman, and B. Jacobs, *J. Appl. Physics* **78**, 4906 (1995).
- ⁵ J. Coombs, A. Jongenelis, W. E. Spiekman, and B. Jacobs, *J. Appl. Physics* **78**, 4918 (1995).
- ⁶ J. Solis, C. Alfonso, S. Hyde, N. Barry, and P. French, *Phys. Rev. Letter* **76**, 2519 (1996).
- ⁷ J. Keirsse *et al.*, *J. Non-Cryst. Solids* **326–327**, 430 (2003).
- ⁸ B. Bureau *et al.*, *J. Non-Cryst. Solids* **345(346)**, 276 (2004).
- ⁹ A. Greer, Lindsay, and N. Mathur, *Nature* **437**, 1246 (2005).
- ¹⁰ P. K. Dwivedi *et al.*, *AIP conf Peoc.* **1349**, 555 (2011).
- ¹¹ I. Think and K. Tanaka, *Phys. Rev. B* **39**, 1270 (1989).
- ¹² S. K. Srivastava, P. K. Dwivedi, and A. Kumar, *Physica B* **183**, 409 (1993).
- ¹³ Z. Wang, C. Tu, Y. Li, and Q. Chen, *J. Non-Cryst. Solids* **191**, 132 (1995).
- ¹⁴ R. Chander and R. Thangaraj, *Chalcogenide Letters* **5**, 229 (2008).
- ¹⁵ V. Vassilev, T. Hristova-Vasileva, and L. Aljihmani, *Chalcogenide Letters* **5**, 39 (2008).
- ¹⁶ A. Dahshan and K. A. Aly, *Acta Mater.* **56**, 4869 (2008).
- ¹⁷ K. A. Aly, A. A. Othman, and A. M. Abousehly, *J. Alloys Compd.* **467**, 417 (2009).
- ¹⁸ A. K. Singh, N. Mehta, and K. Singh, *Philosophical Magazine Letters* **90**, 201 (2010).
- ¹⁹ S. Kumar, K. Singh, and N. Mehta, *Philosophical Magazine Letters* **90**, 547 (2010).
- ²⁰ S. Kumar and K. Singh, *Thermochimica Acta* **528**, 32 (2012).
- ²¹ S. Kumar and K. Singh, *Physica B* **406**, 1519 (2011).
- ²² S. Kumar and K. Singh, *J. Material Science* **47**, 3949 (2012).
- ²³ K. Sedeek *et al.*, *Materials Chemistry and Physics* **85**, 20 (2004).
- ²⁴ S. Gautam *et al.*, *Journal of Non-Crystalline Solids* **353**, 1315 (2007).
- ²⁵ N. A. Hegab *et al.*, *Journal of Alloys and Compounds* **477**, 925 (2009).
- ²⁶ A. A. Shaheen *et al.*, *Current Applied Physics* **11**, 492 (2011).
- ²⁷ A. Sharma, N. Mehta, and A. Kumar, *J Mater Science* **46**, 4509 (2011).
- ²⁸ I. S. Yahia *et al.*, *Physica B* **407**, 2476 (2012).
- ²⁹ I. S. Ram *et al.*, *Journal of Alloys and Compounds* **552**, 480 (2013).
- ³⁰ A.N. Upadhyay *et al.*, *Materials Letters* **136**, 445 (2014).
- ³¹ K. Funke *et al.*, *Solid State Ionics* **154–155**, 65 (2002).
- ³² G. Lucovsky, *J. Non-Cryst. Solids* **97–98**, 155 (1987).
- ³³ R.M. Mehra, G. Kaur, and P.C. Mathur, *J. Mater. Sci.* **26**, 3433 (1991).
- ³⁴ K. Shimakawa and S. Nitta, *Phys. Rev. B* **17**, 3950 (1978).
- ³⁵ N. Afify, *Physica B* **179**, 48 (1992).
- ³⁶ R.K. Shukla, S. Swarup, A. Kumar, and A.N. Nigam, *Semicond Sci Technol* **4**, 68 (1989).
- ³⁷ S. Murugavel and M. Upadhyay, *Journal of the Indian Institute of Science* **91:2**, 303 (2011).
- ³⁸ A. K. Jonscher, *Nature* **267**, 673 (1977).
- ³⁹ N. F. Mott and E. A. Davis, *Electronic Processes in Non-Crystalline Materials* (Clarendon Press, Oxford, 1970).
- ⁴⁰ N. F. Mott and E. A. Davis, *Philosophical Magazine* **22**, 903 (1970).
- ⁴¹ M. A. M. Khan *et al.*, *Material Research Bulletin* **45**, 727 (2010).
- ⁴² K. L. Bhatia *et al.*, *Semicond. Sc. Technol* **10**, 65 (1995).
- ⁴³ J. E. Baurrelle, *J. Phys. Chem. Solids* **30**, 2657 (1969).
- ⁴⁴ H. Lee *et al.*, *Materials Science and Engineering B* **119**, 196 (2005).